

Supplementary Material

for the paper

Band gap engineering of donor-acceptor co-crystals by complementary two-point hydrogen bonding

Nathan Yee, Afshin Dadvand, Dmitrii F. Perepichka*

Table of Content

1. Methods	S2
2. Frontier orbital topologies of H-bonded complexes	S2
3. Solution absorption spectra of donors	S3
4. Vis-NIR absorption spectra of complexes in solution	S4
5. Diffuse reflectance spectra of solid complexes	S5-6
6. IR spectroscopic data	S6
7. IR and Vis-NIR characterization of films of 1e	S6
8. DFT calculation table for complexes of 2 and H-DIP	S7
9. Optimized geometries for complex 1d	S7
10. Crystal structures of 1e	S8
11. PXRDs of complexes 1a-f	S8
12. Synthesis of donor and acceptor components	S9-10
13. NMR spectra	S11-16

* N.Yee, A. Dadvand, D. F. Perepichka

Department of Chemistry and Centre for Self-Assembled Chemical Structures
McGill University, Montreal, Qc H3A 0B8 (Canada)
E-mail:dmitrii.perepichka@mcgill.ca

Methods

Solution UV/vis measurements were recorded on a JASCO V-670 spectrophotometer (Note: **1e** was performed in benzonitrile due to insufficient solubility in other organic solvents). Diffuse reflectance measurements were performed on an Agilent CARY 5000 spectrometer. FT-IR spectra were obtained on a Perkin Elmer Spectrum II FT-IR Spectrometer. Cyclic voltammetry measurements were performed using a CHI-760C Electrochemical Workstation.

Thin-film FETs (TF-FETs) were fabricated bottom-contact bottom-gate configurations (with symmetric Au electrodes as drain and source) by vacuum deposition on pre-patterned substrates (Gen4 from Fraunhofer) and the performance of the resulting OFETs was measured in vacuum and ambient atmosphere using Keithley 4200-SCS.

Approximately, 50 nm thin-film (nominal thickness) of **1** and **1e** were grown by vacuum deposition (5×10^{-7} mbar, deposition rate of 0.1–0.3 Å/sec, evaporation temperature of 150 °C, substrates kept at room temperature) on octyltrichlorosilane (OTS) treated SiO₂/Si wafer (thermally grown 200 nm SiO₂ of heavily n-doped (Sb) Si, $\rho \approx 0.01$ Ohm cm; $C = 1.8 \times 10^{-8}$ F/cm²). The reported OFETs figures of merit are the average of 20 devices.

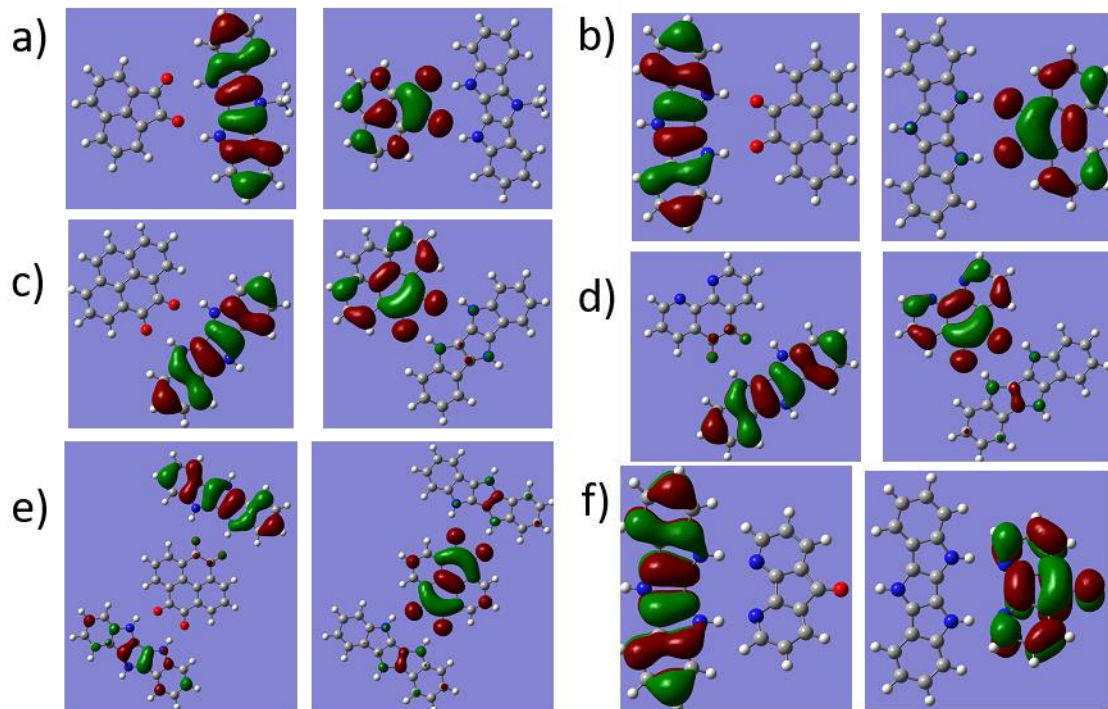


Figure S1 DFT (B3LYP/6-31G(d)) calculated frontier orbital topologies of H-bonded complexes **a-f** with DIP.

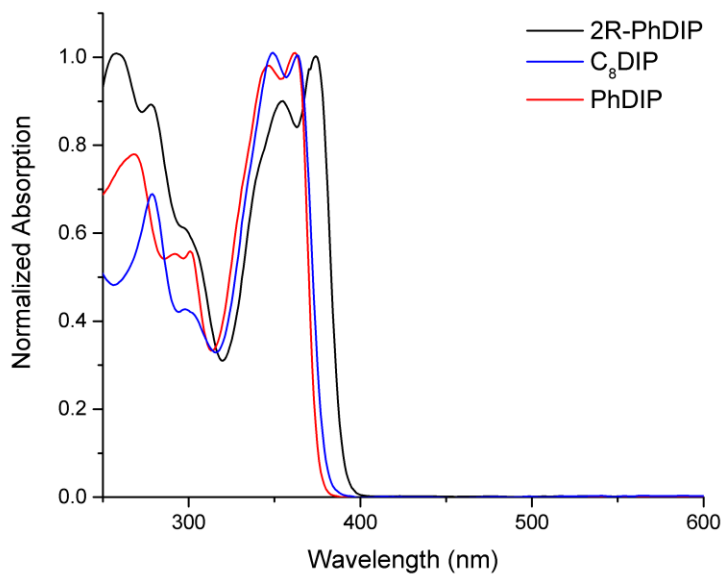


Figure S2 Solution absorption of donors **1**, **1'**, and **2** in CH₂Cl₂.

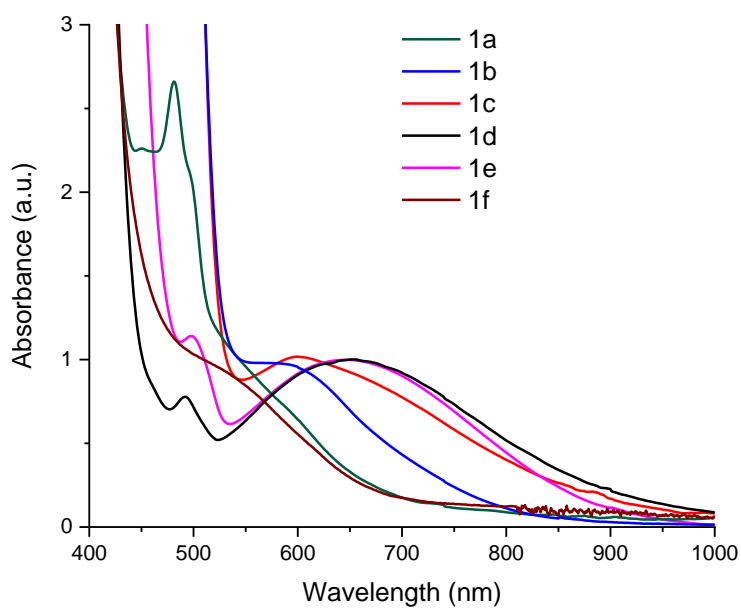


Figure S3 Absorption spectra of solutions **1** with acceptors **a-f** in CH₂Cl₂ (8 mM).

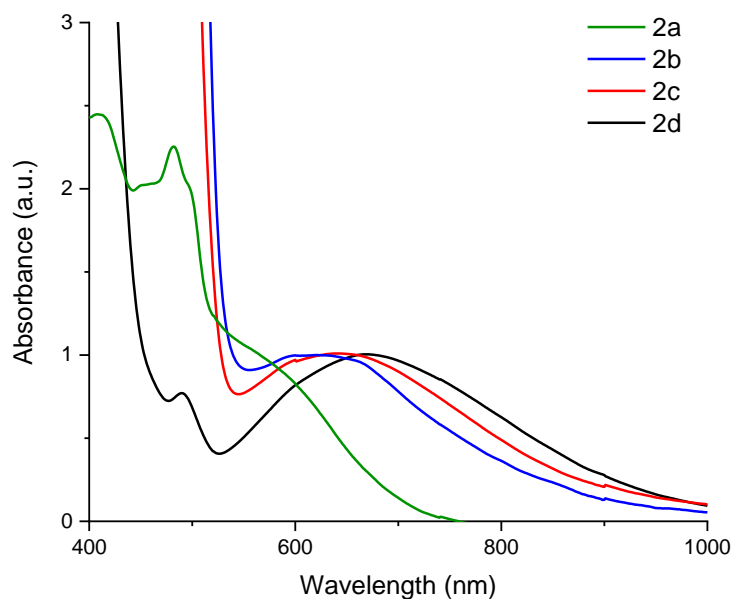


Figure S4 Absorption spectra of solutions **2** with acceptors **a-d** in CH_2Cl_2 (8 mM).

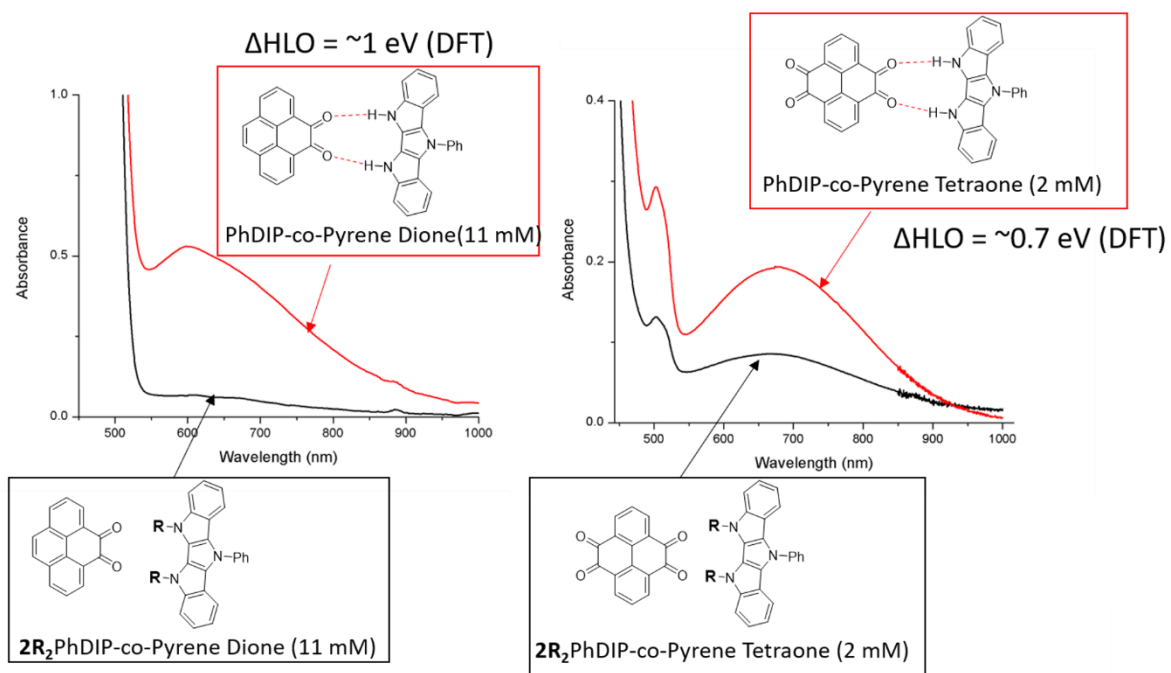


Figure S5. Absorption spectra of solutions **1c** and **1'e** (11 mM, left), **1e** and **1'e** (2mM, right) in CH_2Cl_2 .

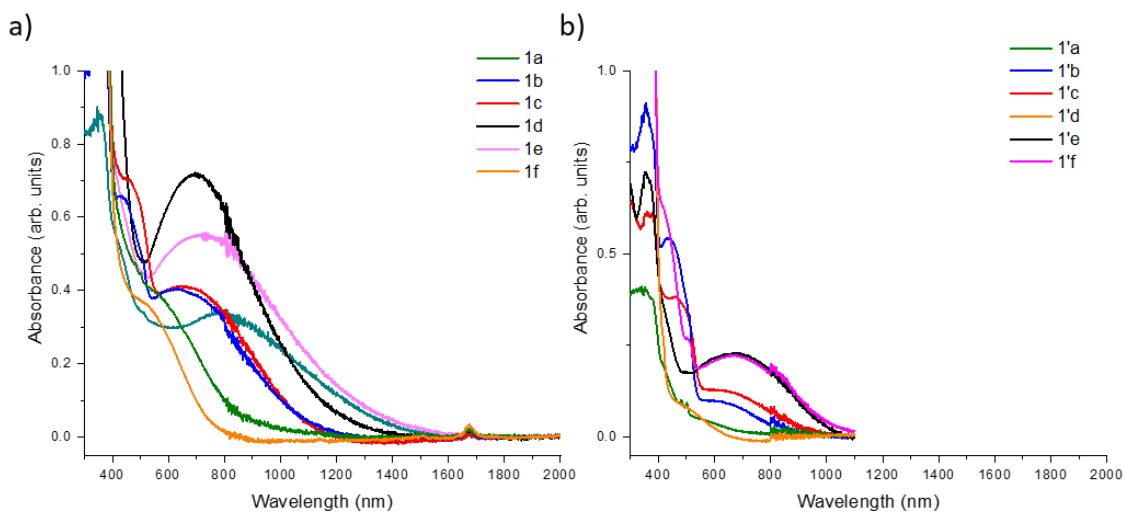


Figure S6 Solid state absorption spectra (diffuse reflectance) of (a) **1a-1f** and (b) **1'a-1'f** in KBr.

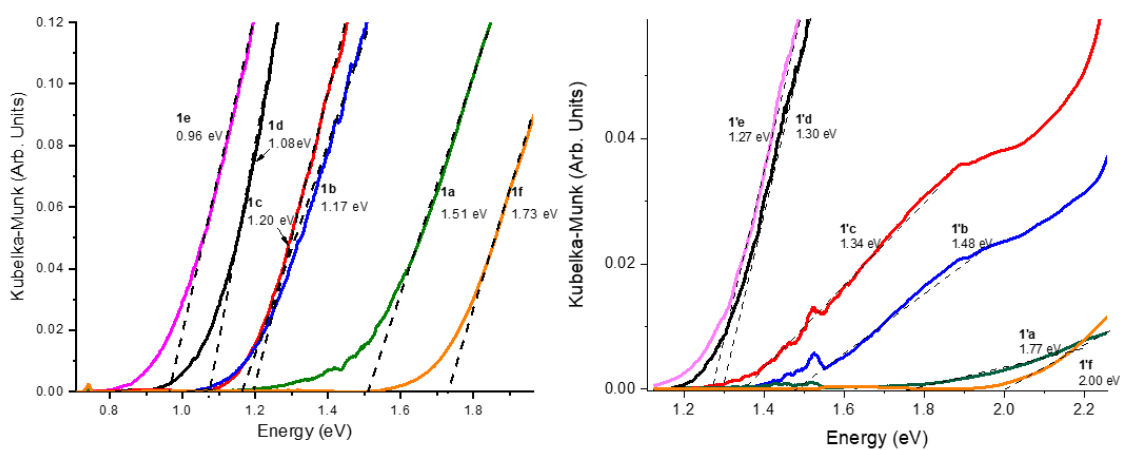


Figure S7 Kubelka Munk plots for complexes of **1a-1f** and **1'a-1'f**. Diffuse reflectance values were converted to Kubelka-Munk using the equation $\frac{(1 - \frac{Reflectance}{100})^2}{Scattering\ factor}$ and plotted against energy $E = \frac{1240}{\lambda}$. Additional details can be found in ref ¹.

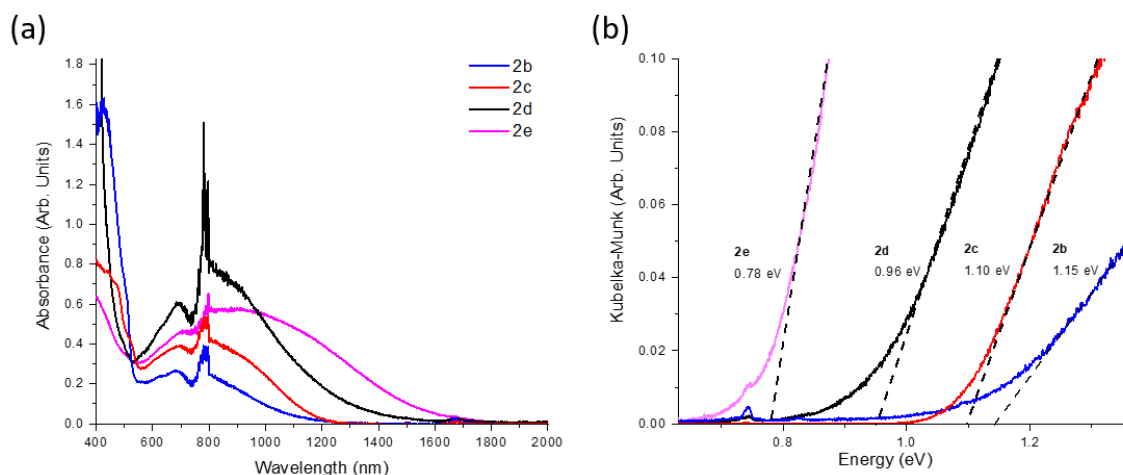


Figure S8 (a) Diffuse reflectance spectra of **2b -2e**. (b) Corresponding Kubelka-Munk plots.

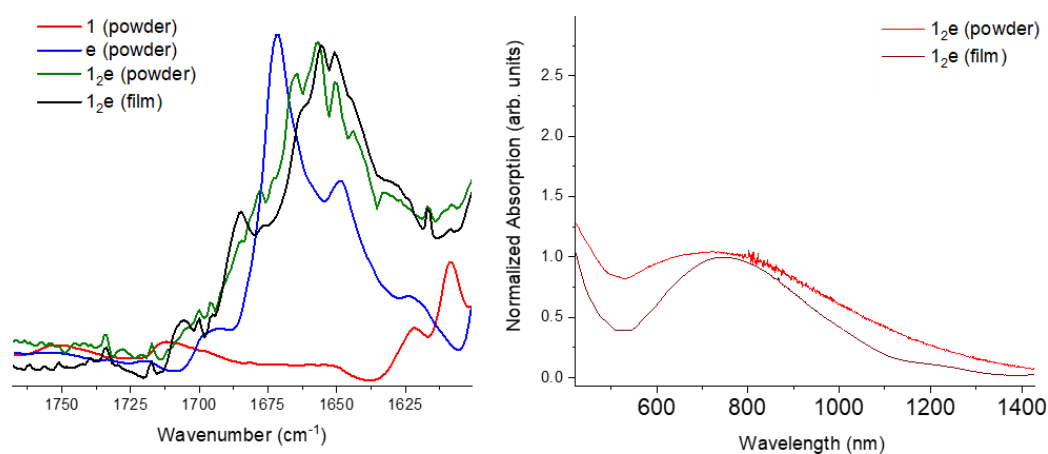


Figure S9 IR spectra for **1, e, 12e** (magnified in carbonyl stretching region) and Vis-NIR spectra for **12e** (powder and film).

Table S1. Shifts in C=O and N-H frequency upon H bonding.

Complex	$\Delta\nu$ C=O (cm ⁻¹)	$\Delta\nu$ N-H (cm-1)
1a	-3	37
1b	-12	35, -84
1c	-6	58, -73
1d	-23	48, -37
1e	-13	52, -104
1f	N/A	6
2c	-9	-111
2e	-30	-37

Table S2 DFT (B3LYP/6-31G(d)) calculations of HOMO, LUMO, HOMO-LUMO gap (HLG), and Δ HLG for H-bonded complexes of **2** with acceptors **a-f**, HOMO of donor (HOMO^D) and LUMO of acceptors (LUMO^A). The octyl group in **2** was replaced with ethyl for simplicity.

Acceptor	a	b	c	d	e	f
HOMO ^D	-4.55	-4.55	-4.55	-4.55	-4.55	-4.55
HOMO ^{D-A} (eV)	-4.05	-4.14	-4.11	-4.34	-4.47	-4.21
Δ HOMO (eV) ^[a]	0.50	0.31	0.44	0.21	0.08	0.34
LUMO ^A	-2.61	-2.98	-2.96	-3.32	-3.35	-2.66
LUMO ^{D-A} (eV)	-3.33	-3.57	-3.55	-3.78	-4.00	-3.19
Δ LUMO (eV) ^[a]	-0.72	-0.59	-0.59	-0.44	-0.65	-0.53
HLG ^{D-A}	0.72	0.57	0.56	0.56	0.47	1.02
Δ HLG ^[b]	1.22	1.00	1.23	0.67	0.73	0.87

[a] Shift vs. HOMO^D (or LUMO^A); [b] Difference between HLG of a complex and the HOMO^D-LUMO^A off-set of the individual components

Table S3 DFT (B3LYP/6-31G(d)) calculations of binding energy (E_b), HOMO, LUMO, HOMO-LUMO gap (HLG), and Δ HLG for H-bonded complexes of unsubstituted DIP with acceptors **a-g**, HOMO of donor (HOMO^D) and LUMO of acceptors (LUMO^A).

Acceptor	a	b	c	d	e	f
E_b (kcal/mol)	11.4	11.1	11.3	11.1	24.3 ^[c]	10.7
HOMO ^D	-4.58	-4.58	-4.58	-4.58	-4.58	-4.58
HOMO ^{D-A} (eV)	-4.02	-4.13	-4.12	-4.34	-4.50	-4.24
Δ HOMO (eV) ^[a]	0.52	0.41	0.42	0.20	0.04	0.30
LUMO ^A	-2.61	-2.98	-2.96	-3.32	-3.35	-2.66
LUMO ^{D-A} (eV)	-3.33	-3.59	-3.58	-3.82	-4.05	-3.21
Δ LUMO (eV) ^[a]	-0.72	-0.61	-0.62	-0.50	-0.70	-0.55
HLG ^{D-A}	0.69	0.54	0.54	0.52	0.45	1.03
Δ HLG ^[b]	1.24	1.02	1.04	0.70	0.74	0.85

[a] Shift vs. HOMO^D (or LUMO^A); [b] Difference between HLG of a complex and the HOMO^D-LUMO^A off-set of the individual components; [c] Energy is for 2:1 binding (**1_{2e}**).

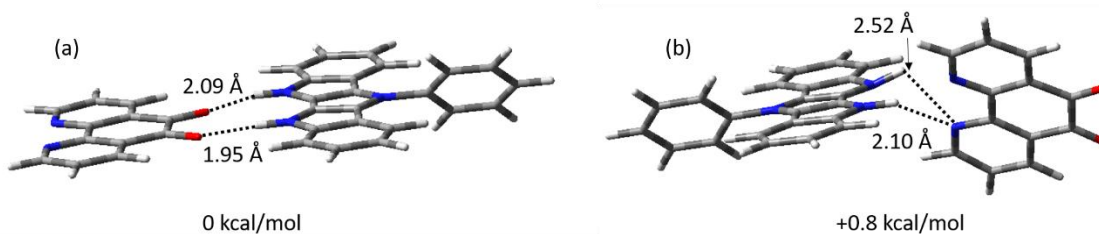


Figure S10 DFT (B3LYP/6-31G(d)) calculated optimized geometry for complex **1d** with (a) **1** H-bonded to carbonyl groups of **d** (b) **1** H-bonded to aza nitrogen atoms of **d**.

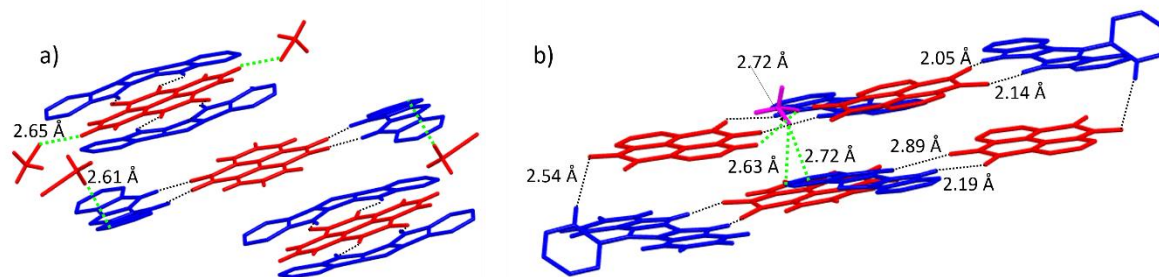


Figure S11 Crystal structure polymorphs of **12e** (2:1 binding, a) and **1e** (1:1 binding, b) with the solvating MeCN molecules.

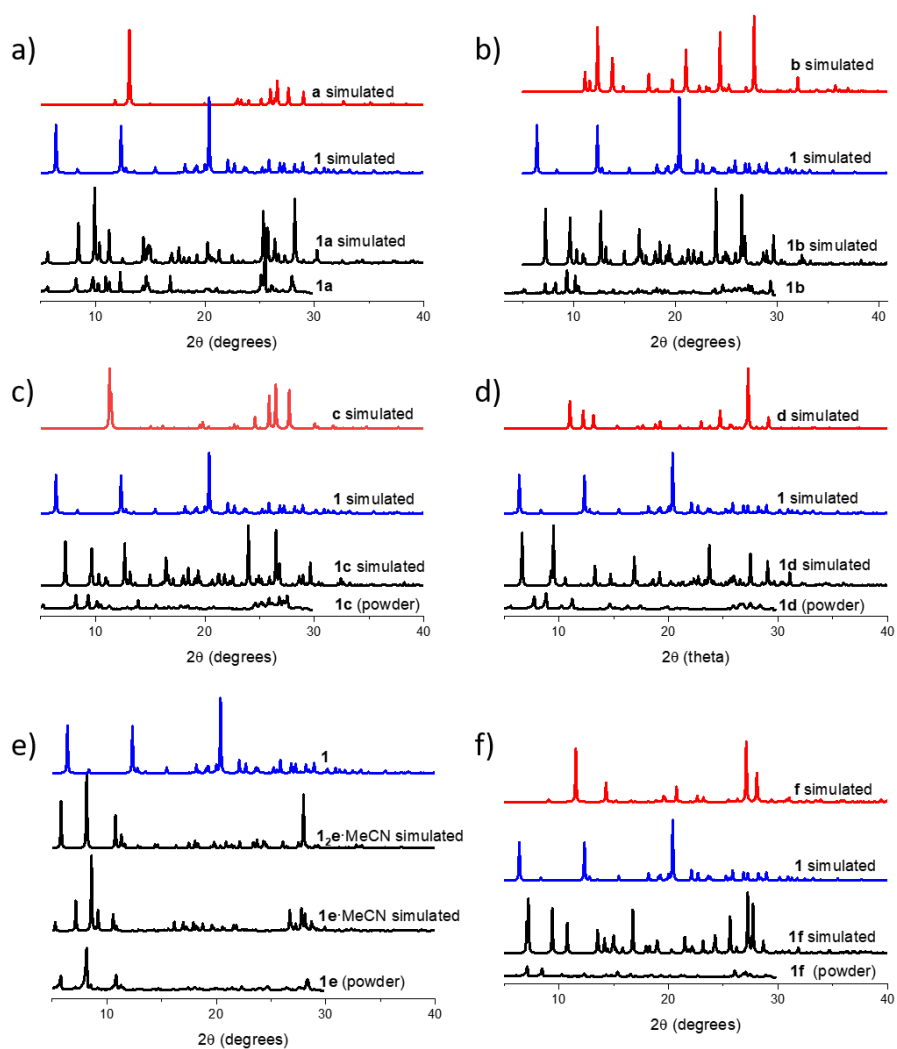


Figure S12 Comparison of PXRDs of complexes **1a-f** prepared by precipitation vs. those simulated from single crystal structures of corresponding complexes and their individual components.

Synthesis

2,5-bis(2-nitrophenyl)-1-phenylpyrrole, 11-phenyl-6,11-dihydropyrrolo[3,2-b:4,5-b']diindole (**1**), 2,5-bis(2-nitrophenyl)-1-octylpyrrole, 11-octyl-6,11-dihydropyrrolo[3,2-b:4,5-b']diindole (**2**), and 5,6-diethyl-11-phenyl-6,11-dihydropyrrolo[3,2-b:4,5-b']diindole (**1'**) were synthesized according to ref. ²; spectral data matched that reported in literature. Pyrene tetraone (**e**) was synthesized according to a literature procedure,³ spectral data matched that reported in literature.

1-phenylpyrrole was prepared according to a modified literature procedure;⁴ NMR spectral data matched that reported in literature. Aniline (1.0 g, 10 mmol) and 2,5-dimethoxytetrahydrofuran (1.1 g, 9.0 mmol) were added to a Schlenk flask and stirred at 120 °C overnight. After cooling to room temperature, the reaction mixture was loaded onto a silica column and purified by column chromatography eluting with hexanes/DCM to yield a white solid (180 mg, 13%). ¹H NMR (400 MHz, CDCl₃): δ (ppm) 7.40-7.46 (4H, m), 7.11 (2H, t, J = 4.4 Hz), 6.36 (2H, t, J = 4 Hz)

2,5-bis(2-nitrophenyl)-1-phenylpyrrole. 1-Phenyl-1H-pyrrole (0.16 g, 1.00 mmol), 2-bromonitrobenzene (0.89 g, 4.00 mmol), Cs₂CO₃ (2.80 g, 8.60 mmol), and acetonitrile (8 mL) were added to a Schlenk flask and stirred at reflux overnight under an atmosphere of argon. After cooling to room temperature, the crude brown mixture was purified by column chromatography on silica gel eluting with a gradient starting from hexanes to a mixture of hexanes/ethyl acetate (10:1) to yield a white solid (166 mg, 40%). ¹H NMR (400 MHz, CDCl₃): δ (ppm) 7.70-7.72 (2H, m), 7.47-7.52 (4H, m), 7.35-7.39 (2H, m), 7.05-7.14 (3H, m), 6.81-6.83 (2H, m), 6.46 (2H, s)

11-phenyl-6,11-dihydropyrrolo[3,2-b:4,5-b']diindole (**1**) 2,5-bis(2-nitrophenyl)-1-phenyl-1H-pyrrole (0.14 g, 0.4 mmol) and triethylphosphite (0.97 g, 5.80 mmol) were added to a Schlenk tube and stirred at 180 °C. After cooling to room temperature, the excess of triethylphosphite and formed triethylphosphonate were removed by distillation under reduced pressure (90 °C, ~10 mbar). The remaining crude material was purified by column chromatography on silica gel eluting with hexanes/DCM to yield a white solid (58 mg, 42%) ¹H NMR (400 MHz, CDCl₃): δ (ppm) 10.03 (2H, s), 7.90-7.91 (2H, m), 7.71-7.75 (2H, m), 7.61 (2H, d, J = 8 Hz), 7.49 (2H, d, 8 Hz), 7.43-7.5 (1H, m), 6.99-7.02 (2H, m)

N-Octylpyrrole was prepared according to a modified literature procedure⁵; spectral data matched that reported in literature NaH (10.7 g, 0.45 mol) and anhydrous THF (75 mL) were added to 250 mL round bottom flask equipped with a stir bar and reflux condenser. Pyrrole (10 g, 0.15 mol) was added slowly via syringe and the mixture was stirred at room temperature for two hours. 1-Bromooctane (45 mL, 0.20 mol) was measured with a syringe and added slowly and the solution which was stirred at reflux overnight. After cooling to room temperature, the mixture was diluted with water, extracted twice with ethyl acetate, and washed with water, dried over MgSO₄, and the solvent removed by rotary evaporation. The compound was purified by column chromatography eluting with hexanes yielding a colorless oil (3.0 g, 11%). ¹H NMR (400 MHz, CDCl₃) δ (ppm) 6.65 (2H, m), 6.13 (2H, m), 3.86 (2H, t, J = 7.2 Hz), 1.75 (2H, m), 1.24-1.27 (12H, m), 0.88 (3H, t, J = 7 Hz)

2,5-bis(2-nitrophenyl)-1-octylpyrrole Octyl pyrrole (1.0 g, 5.6 mmol), Cs₂CO₃ (7.0 g, 22 mmol), 1-bromo-2-nitrobenzene (4.5 g, 22 mmol), acetonitrile (50 mL) were added to a 250 mL two-neck flask equipped with a stir bar and reflux condenser. The solution was purged with argon for 10 minutes and then stirred at reflux overnight. After cooling to room temperature, the solution

was diluted with water (100 mL) and extracted with ethyl acetate (2 x 100 mL), dried over MgSO₄, and the solvent removed under reduced pressure. The crude was loaded onto silica and purified via column chromatography eluting with hexanes to DCM (100% hexanes gradient to 50/50 hexanes:DCM) yielding an orange solid (450 mg, 20%). ¹H NMR (400 MHz, CDCl₃) δ (ppm) 7.93 (2H, d, J = 8 Hz), 7.63-7.62 (2H, m), 7.55-7.53 (4H, m), 7.20 (2H, s), 3.62 (2H, t, J = 7.6 Hz), 1.26-0.85 (12H, m), 0.81(3H, t, J = 7.6 Hz)

11-octyl-6,11-dihydropyrrolo[3,2-b:4,5-b']diindole (2). 2,5-bis(2-nitrophenyl)-1-octylpyrrole (1.6 g, 4.5 mmol) and triethylphosphite (15 mL) were added to a 25 mL Schlenk tube and stirred at reflux for 8 hours. After cooling to room temperature, most of the triethylphosphite was removed by rotary evaporation. The crude was loaded onto silica and purified via column chromatography eluting with hexanes:EtOAc (100% hexanes to 80:20 hexanes:EtOAc). The fractions were combined, and solvent removed by rotary evaporation and filtered yielding a white cotton-like solid with some dark impurities (900 mg, 56%). To remove impurities, hexanes was added, and the suspension was filtered to yield a white cotton-like compound (710 mg, 44%) ¹H NMR (400 MHz, CDCl₃) δ (ppm) 10.66 (2H, s), 7.72 (2H, d, J = 7.6 Hz), 7.39 (2H, d, J = 8 Hz), 7.05-6.99 (4H, m), 4.56 (2H, t, J = 6.6 Hz), 1.87-1.84 (2H, m), 1.27-1.09 (12H, m), 0.74 (3H, t).

5,6-diethyl-11-phenyl-6,11-dihydropyrrolo[3,2-b:4,5-b']diindole (1'). (0.16 g, 1.40 mmol) was added to a Schlenk flask containing **1** (0.16 g, 0.50 mmol) in anhydrous THF (5 mL) and a stir bar. The mixture was stirred under reflux for 1 hour. Bromo-1-octane was added slowly, and the mixture was refluxed overnight. After cooling to room temperature, the mixture was extracted with DCM (x2), washed with water, and dried over MgSO₄. The crude compound was loaded onto silica and purified by column chromatography eluting with a gradient of hexanes/EtOAc (100:0 to 90:10) yielding a white solid, which was suspended in methanol and filtered to yield a white solid (140 mg, 55%). ¹H NMR (500 MHz, CDCl₃) δ (ppm) 7.87 (2H, d, J = 7 Hz), 7.64-7.61 (4H, m), 7.42-7.40 (3H, m), 7.23 (2H, t, J = 7.5 Hz), 7.05 (2H, t, J = 7.5 Hz), 4.46 (4H, t, J = 7.5 Hz), 2.00-1.95 (4H, m), 1.47-1.28 (24 H, m), 0.90-0.87 (3H, t, J = 7 Hz)

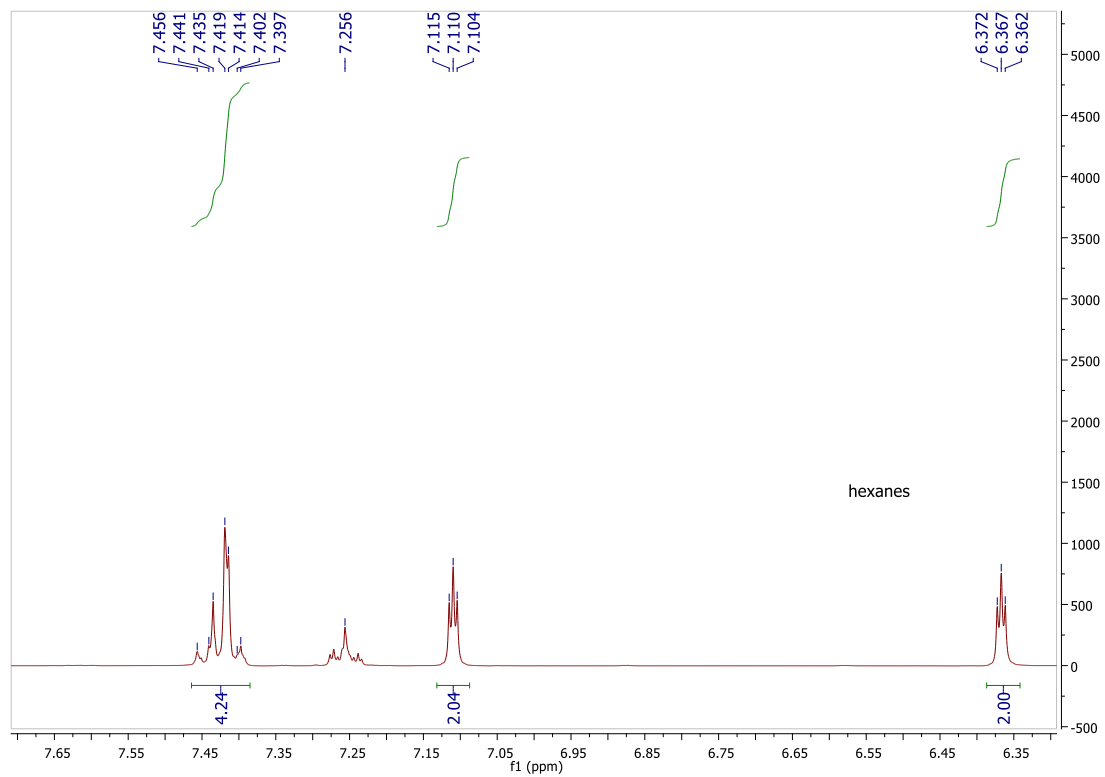
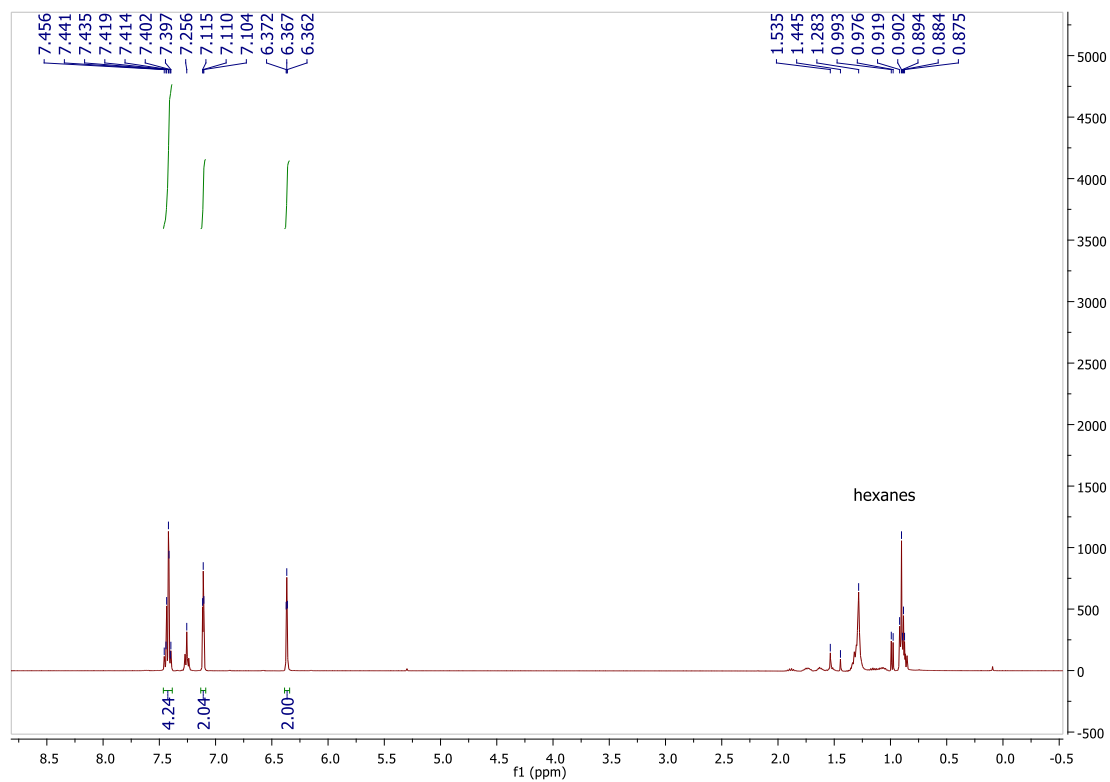


Figure S13 (top) ^1H NMR spectrum of 1-phenylpyrrole (400 MHz, CDCl_3). (bottom) Magnified aromatic region.

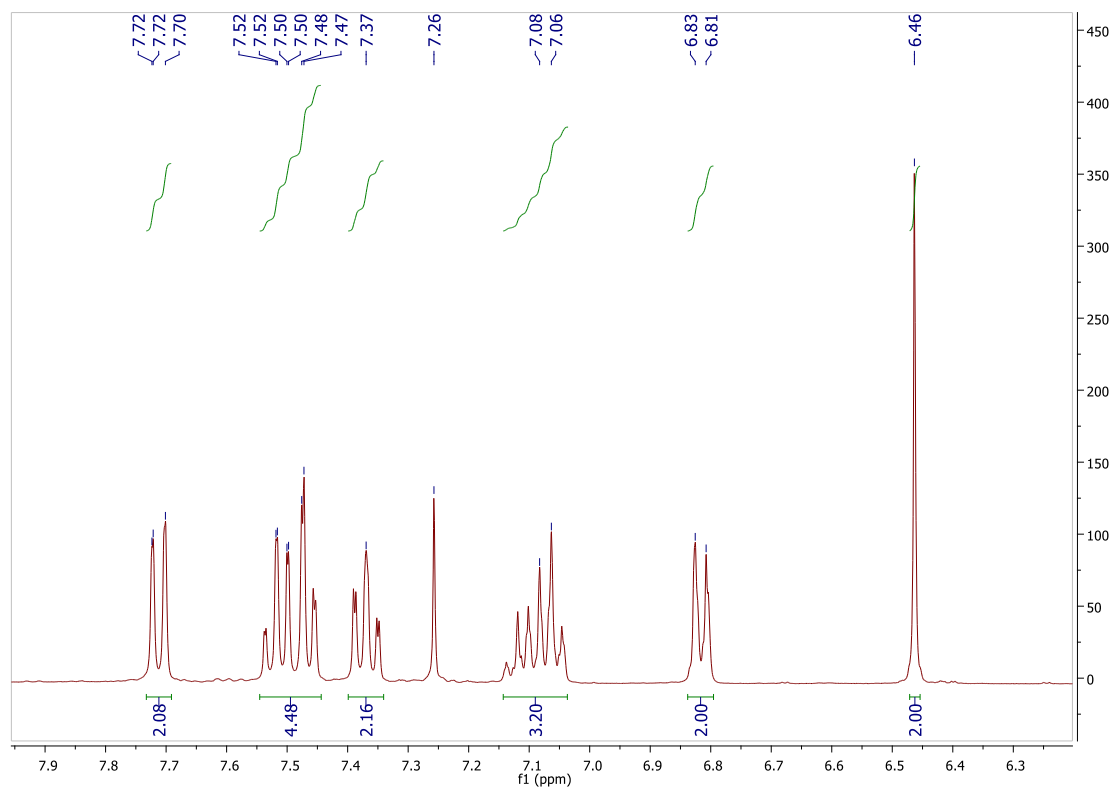
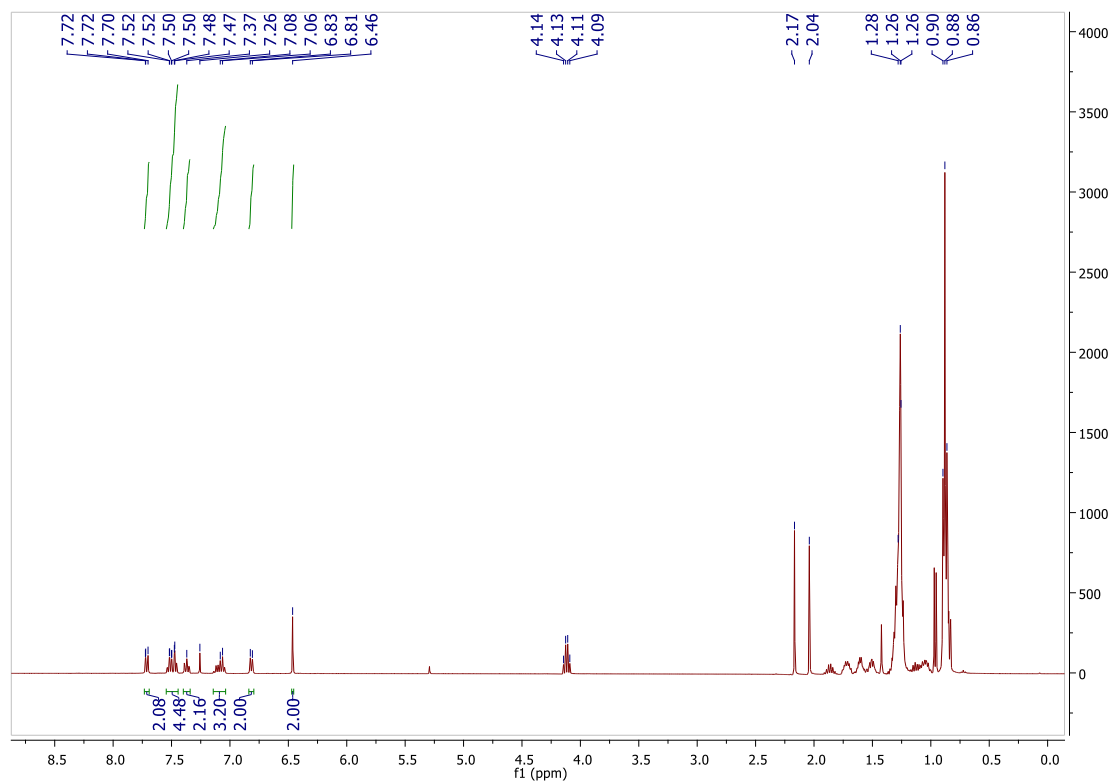


Figure S14 (top) ^1H NMR spectrum of 2,5-bis(2-nitrophenyl)-1-phenyl-1H-pyrrole (400 MHz, CDCl_3). (bottom) Magnified aromatic region

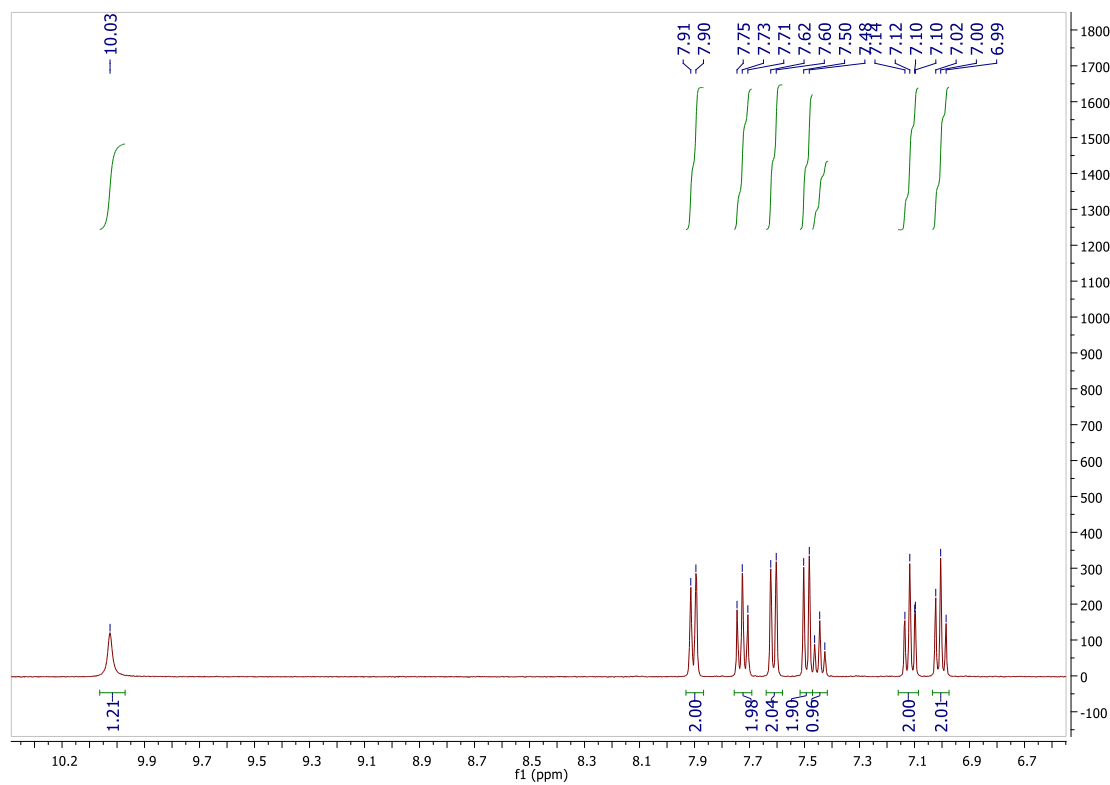
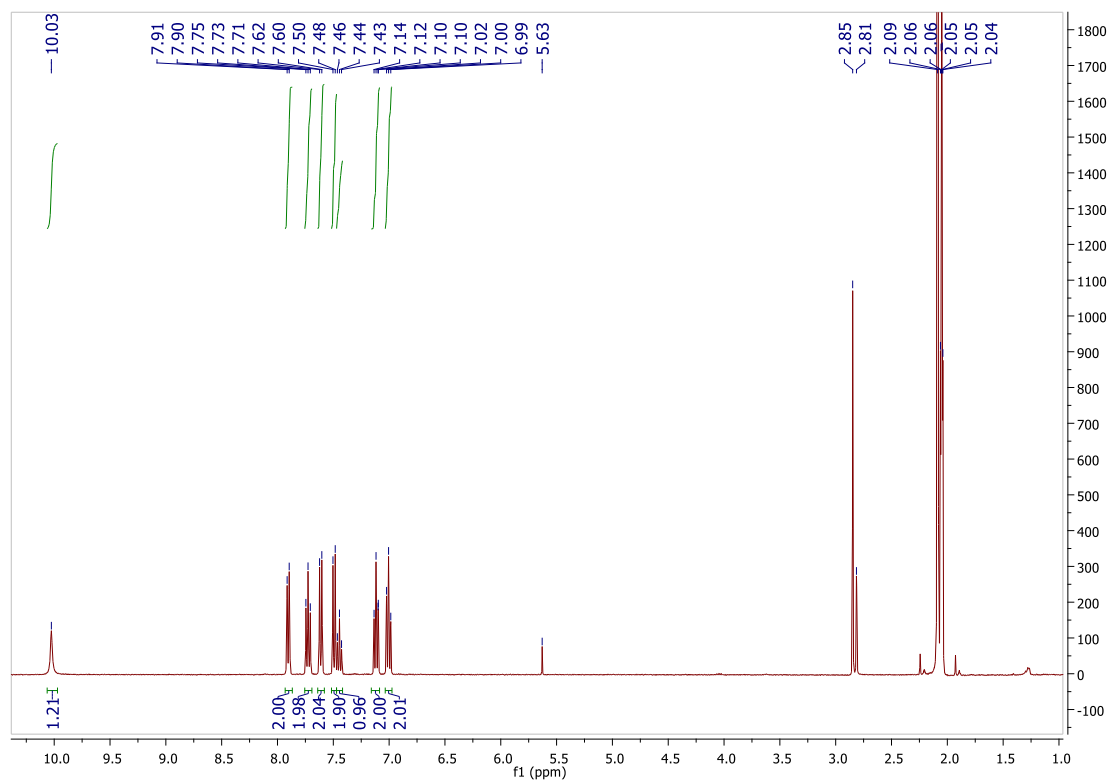


Figure S15 (top) ^1H NMR spectrum of **1** (400 MHz, acetone- d_6). (bottom) Magnified aromatic region.

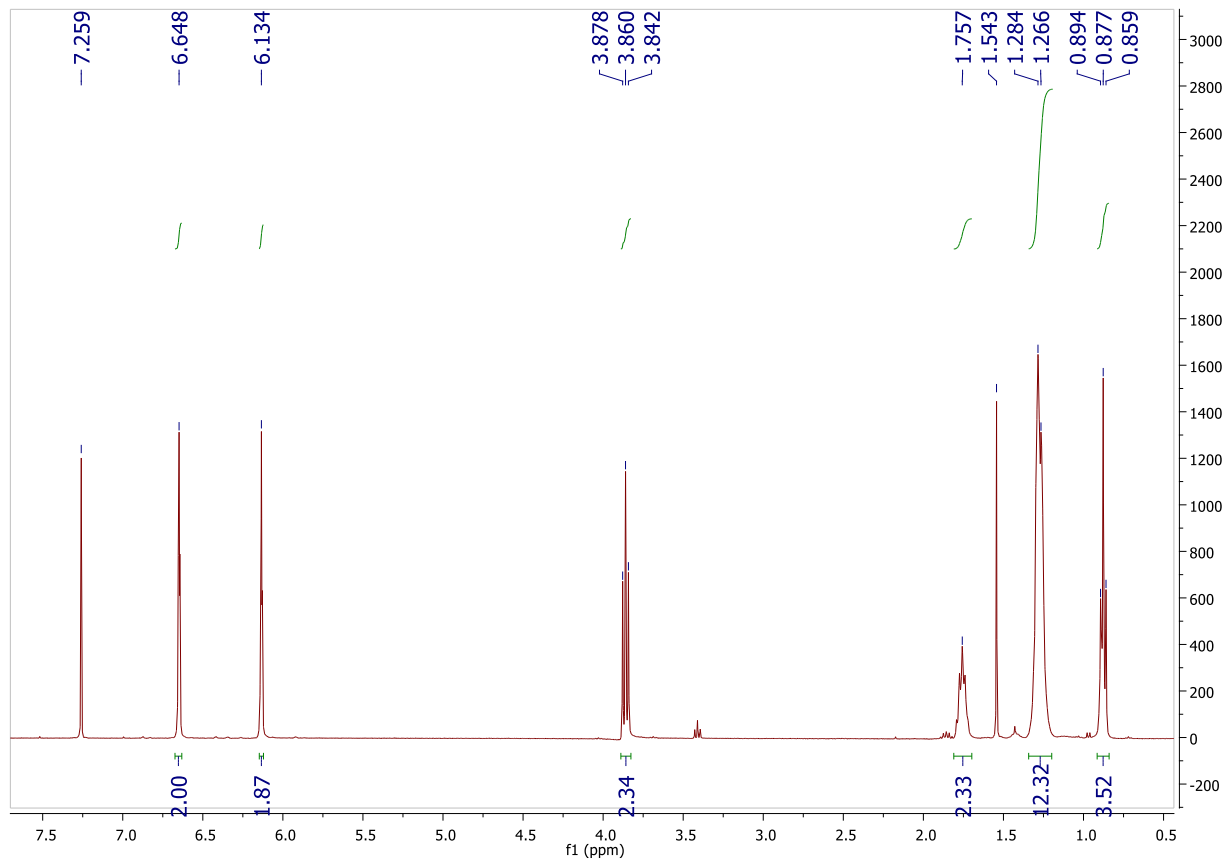


Figure S16 ^1H NMR spectrum of octyl pyrrole (500 MHz, CDCl_3).

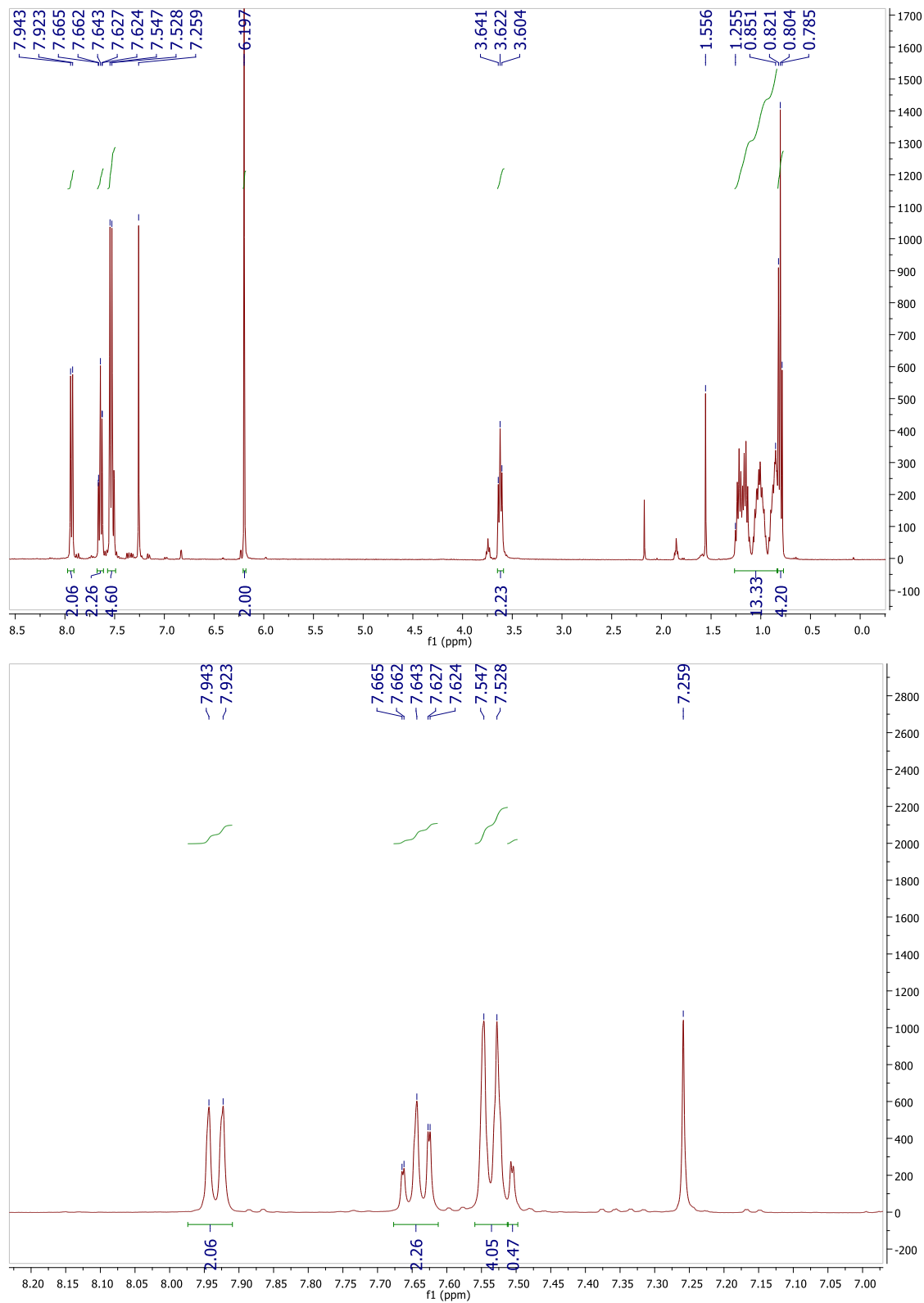


Figure S17 (top) ¹H NMR spectrum of 2,5-bis(2-nitrophenyl)-1-octylpyrrole (500 MHz, CDCl₃). (bottom) Magnified aromatic region

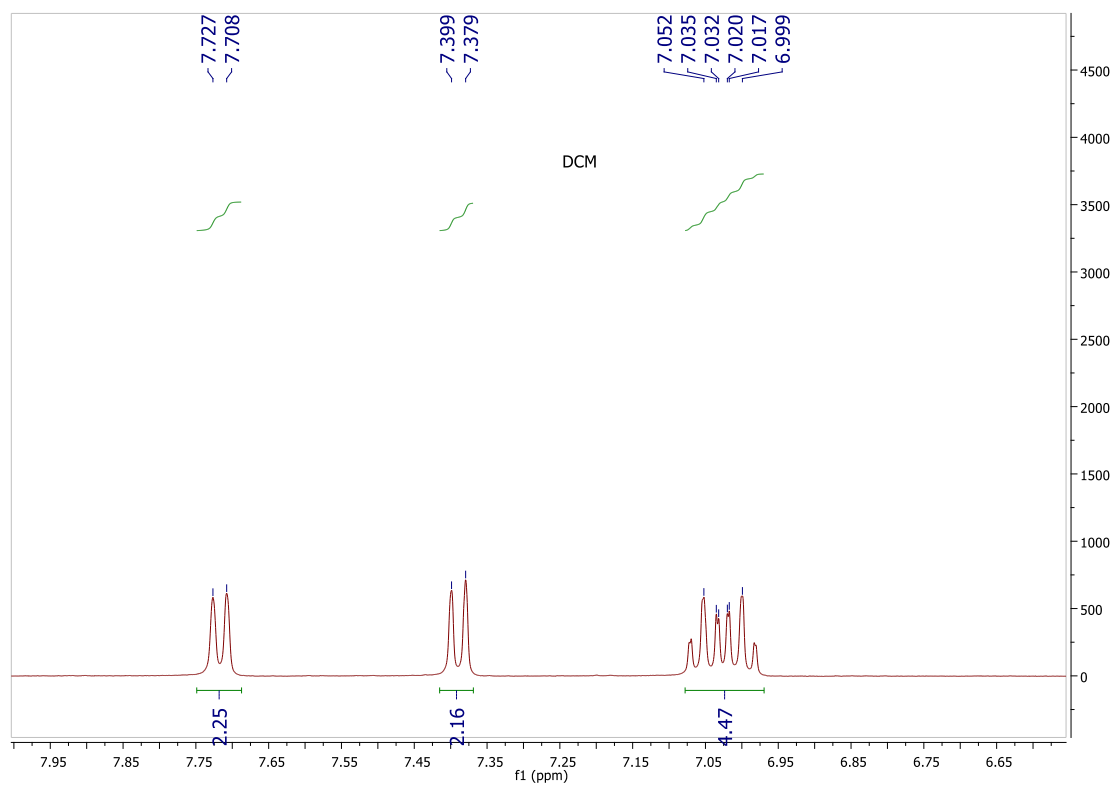
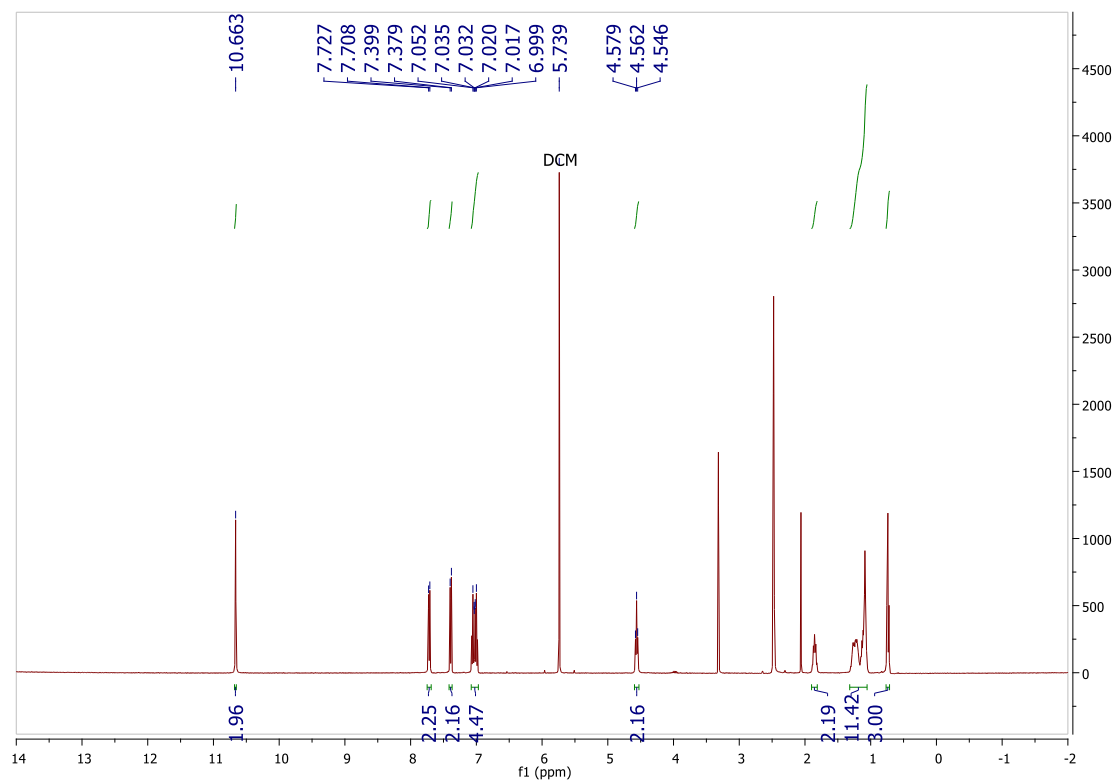


Figure S18 (top) ^1H NMR spectrum of **2** (400 MHz, CDCl_3). (bottom) Magnified aromatic region.

References

1. <https://mmrc.caltech.edu/FTIR/Literature/Diff%20Reflectance/Kubelka-Munk.pdf> (accessed 2020-07-06).
2. M.-J. Jiang, W.-J. Xiao, J.-C. Huang, W.-S. Li and Y.-Q. Mo, *Tetrahedron*, 2016, **72**, 979-984.
3. Y. Liu, T. Shan, L. Yao, Q. Bai, Y. Guo, J. Li, X. Han, W. Li, Z. Wang and B. Yang, *Org. Lett.*, 2015, **17**, 6138-6141.
4. K. Ramesh, S. N. Murthy and Y. V. D. Nageswar, *Synth. Commun.*, 2012, **42**, 2471-2477.
5. M. R. Nateghi, S. Dehghan and M. Shateri-Khalilabad, *International Journal of Polymeric Materials and Polymeric Biomaterials*, 2013, **62**, 648-652.